TECHNICAL MEMORANDUM

NUREG/CR-1814
ANL-CT-81-9

(Distribution
Code: R7)

ARGONNE NATIONAL LABORATORY
9700 South Cass Avenue
Argonne, Illinois 60439

SIMULATION OF STEADY-STATE AND TRANSIENT SODIUM BOILING EXPERIMENTS IN A SEVEN-PIN BUNDLE UNDER FLOW RUNDOWN CONDITIONS BY USING BODYFIT-1FE CODE

by

Brian C-J. Chen and William T. Sha

Components Technology Division

January 1981

Prepared for the

Division of Reactor Safety Research
Office of Nuclear Regulatory Research
U. S. Nuclear Regulatory Commission
Washington, D. C. 20555

NRC FIN No. A2045

SIMULATION OF STEADY-STATE AND TRANSIENT SODIUM BOILING EXPERIMENTS IN A SEVEN-PIN BUNDLE UNDER FLOW RUNDOWN CONDITIONS BY USING BODYFIT-1FE CODE

by

Brian C-J. Chen and William T. Sha

ABSTRACT

A seven-pin rod bundle under flow rundown conditions was simulated by using the computer code BODYFIT-1FE (Boundary-Fitted Coordinate System - 1 phase, Fully-Elliptic). In this code, the complicated rod bundle configuration is first transformed into rectangular geometry with uniform meshes. The transformed governing equations for all the thermal-hydraulic variables are then solved. The results of the simulation are presented here. All the predicted values agree favorably with the measured data.

NRC FIN #

A2045

Title

3-D Time-dependent Code Development

TABLE OF CONTENTS

LIST OF FIGURES

LIST OF FIGURES (CONTD.)

Executive Summary

A 7-pin rod bundle under flow rundown condition was simulated by using the computer code BODYFIT-1FE, which is based on the technique of boundary-fitted coordinate systems. By using this technique, one can transform the complicated rod-bundle configuration into either rectangular or cylindrical coordinates with uniform meshes. Therefore, the boundary conditions at the solid surfaces are accurately represented without any interpolation.

The transformed Navier-Stokes equations are solved by using the finite-difference technique. This procedure provides detailed velocity and temperature distribution. We have used this procedure to simulate the experiment performed at GFK Karlsruhe facility. A brief description of the test condition is given. Physical models used in the simulation are described.

The results of the comparison between the code prediction and the measured value are very encouraging. The agreement can be improved by refining the heat transfer coefficients and physical models. The same experiment was also simulated by COMMIX-1A. The predictions between BODYFIT and COMMIX are fairly close. The BODYFIT-1FE code is a bench mark code since it does not invoke any assumptions and empirical coefficients for laminar flow case. All the conservation equations are rigorously treated except for the case of turbulent flow where a turbulent flow model is needed for the closure of the differential equations. The capability to analyze two-phase flow is to be added into BODYFIT, which will further increase the applicability of the code for various thermal hydraulic analysis.

I. INTRODUCTION

A 7-pin rod bundle under flow rundown condition was simulated by using the technique of boundary-fitted coordinate systems.[1] By using this technique, one can transform the complicated rod-bundle configuration into either rectangular or cylindrical coordinates with uniform meshes. Therefore, the boundary conditions at the solid surfaces are accurately represented without any interpolation. The accuracy of the representation is only limited by the accuracy of the geometric coefficients, which can be easily increased by increasing the number of computational meshes.

A computer program was written to automate the generation of the coordinate system. The detailed equation will be presented in Section II. Once the curvilinear coordinates are generated, the Navier-Stokes equations are solved in the transformed plane using the finite-difference technique. The transformed equations of conservation are given in Section III. This procedure provides detailed velocity and temperature distribution without invoking any assumptions for the laminar flow case. However, for turbulent flow, some empiricism must be employed due to the closure problem of turbulence modelling. A computer code BODYFIT-1FE[2] based on this procedure has been developed. We have used BODYFIT-1FE to simulate the experiment performed at GFK Karlsruhe facility.[3] A brief description of the test condition is given in Section IV. Physical models used in the simulation are described in Section V. This includes the fuel pin model and the grid resistance model. Comparison between the experimental measurements and the code predictions are given in Section VI. Final remarks and conclusions are given in Section VII.

II. COORDINATE TRANSFORMATION

The technique of boundary-fitted coordinate systems is based on an automated numerical generation of a general curvilinear coordinate system having a coordinate line coincident with each boundary of a general multiconnected region containing any number of bodies with arbitrary shapes. This procedure does not use conformal transformation and consequently is not limited to two dimensions. It can also be generalized to cases with time dependent boundaries. The curvilinear coodinates are generated as the solution of a set of elliptic partial differential equations with Dirichlet boundary conditions, one coordinate being specified to be constant on each boundary segment, with monotonic variations of the other coordinate being specified along the boundaries.

Let (x,y) be the coordinate variable in the physical plane and (ξ,η) in the transformed plane. The coordinate mesh is then generated by numerically solving a Laplacian equation

$$\xi_{xx} + \xi_{yy} = 0 \tag{1}$$

$$\eta_{xx} + \eta_{yy} = 0 \tag{2}$$

with the boundary conditions

$$\begin{bmatrix}\xi\\ \eta\end{bmatrix} = \begin{bmatrix}\xi_1\ (x,y)\\ \eta_1\end{bmatrix} \quad , \quad [x,y] \in \Gamma_1$$

$$\begin{bmatrix}\xi\\ \eta\end{bmatrix} = \begin{bmatrix}\xi_2\ (x,y)\\ \eta_2\end{bmatrix} \quad , \quad [x,y] \in \Gamma_2 \tag{3}$$

on each of the boundaries Γ_1 and Γ_2. The subscripts in Eq. (1) and (2) represent second order partial derivatives.

Frequently, it is more convenient to solve the inverse of (1) and (2), because the boundaries can be more easily described. The equations are written in terms of x and y as dependent variables, as follows.

$$\alpha\, x_{\xi\xi} - 2\beta x_{\xi\eta} + \gamma x_{\eta\eta} = 0 \tag{4}$$

$$\alpha\, y_{\xi\xi} - 2\beta y_{\xi\eta} + \gamma y_{\eta\eta} = 0 \tag{5}$$

with the boundary conditions

$$\begin{bmatrix} x \\ y \end{bmatrix} = \begin{bmatrix} f_1(\xi,\eta_1) \\ f_2(\xi,\eta_1) \end{bmatrix}, \quad [\xi,\eta_1] \in \Gamma_1^*$$

$$\begin{bmatrix} x \\ y \end{bmatrix} = \begin{bmatrix} g_1(\xi,\eta_2) \\ g_2(\xi,\eta_2) \end{bmatrix} \quad [\xi,\eta_2] \in \Gamma_2^* \tag{6}$$

where α, β, γ are the transformation coefficents, given by

$$\begin{aligned} \alpha &\equiv x_\eta^2 + y_\eta^2 \\ \beta &\equiv x_\xi x_\eta + y_\xi y_\eta \\ \gamma &\equiv x_\xi^2 + y_\xi^2 \end{aligned} \tag{7}$$

Γ_1^* and Γ_2^* are the transformed boundaries. In multiboundary problems, there are several of these boundary conditions that must be specified.

Equations (4) and (5) are numerically solved using SOR techniques. The solution of the equations is the specification of (x, y) coordinates at discrete (ξ,η) points in the transformed plane. These coordinates are used in the BODYFIT code for solving the transformed equations of conservation.

III. EQUATION OF CONSERVATION

In this section, we only present the transformed continuity equation and the momentum equation to illustrate the character of the transformed equations. The complete set of transformed equations is given in Reference 2.

In the rectangular coordinate system, the governing equations are given as follows.

Mass Conservation

$$\int_V \frac{\partial \rho}{\partial t}\, dV + \int_{S_x} \rho u\, dydz + \int_{S_y} \rho v\, dxdz + \int_{S_z} \rho w\, dxdy = 0$$

X-Momentum

$$\int_V \frac{\partial (\rho u)}{\partial t}\, dV + \int_{S_x} \rho uu\, dydz + \int_{S_y} \rho uv\, dxdz + \int_{S_z} \rho uw\, dxdy$$

$$= \int_{S_x} \Sigma_{11}\, dydz + \int_{S_y} \Sigma_{12}\, dxdz + \int_{S_z} \Sigma_{13}\, dxdy$$

$$- \int_{S_x} p\, dydz + \int_V \rho g_x\, dV$$

where:

ρ = density

u = velocity in x-direction

v = velocity in y-direction

w = velocity in z-direction

Σ_{ij} = viscous stress acting in i-direction on the surface normal to j-direction

p = pressure

g_x = gravity in x-direction

In the boundary-fitted coordinate system, the governing equations are as follows.

Mass conservation

$$\int_V J \frac{\partial \rho}{\partial t} dV' + \int_{S_\xi} \rho \tilde{u} \frac{1}{a} d\eta d\zeta + \int_{S_\eta} \rho \tilde{v} \frac{1}{a} d\xi d\zeta + \int_{S_\zeta} \rho \tilde{w} J_{12} d\xi d\eta = 0$$

x-momentum

$$\int_V J \frac{\partial (\rho u)}{\partial t} dV' + \int_{S_\xi} \frac{1}{a} \rho u \tilde{u} d\eta d\zeta + \int_{S_\eta} \frac{1}{a} \rho u \tilde{v} d\xi d\zeta + \int_{S_\zeta} J_{12} \rho u \tilde{w} d\xi d\eta = - \int_{S_\xi} \frac{1}{a} y_\eta P \, d\eta d\zeta + \int_{S_\eta} \frac{1}{a} y_\xi P \, d\xi d\zeta + \frac{1}{Re} \int_{S_\xi} \frac{1}{a} \tilde{\Sigma}_{11} d\eta d\zeta + \frac{1}{Re} \int_{S_\eta} \frac{1}{a} \tilde{\Sigma}_{12} d\xi d\zeta + \frac{1}{Re} \int_{S_\zeta} J_{12} \tilde{\Sigma}_{13} d\xi d\eta + \frac{1}{F^2} \int_V J(\rho - \rho_s) g_x dV'$$

The variables with the overhead tilde are the transformed variables defined as follows.

$$\tilde{u} = y_\eta u - x_\eta v$$

$$\tilde{v} = - y_\xi u + x_\xi v$$

$$\tilde{w} = w$$

$$\tilde{\Sigma}_{11} = y_\eta \Sigma_{11} - x_\eta \Sigma_{12}$$

$$\tilde{\Sigma}_{12} = - y_\xi \Sigma_{11} + x_\xi \Sigma_{12}$$

$$\tilde{\Sigma}_{13} = \Sigma_{13}$$

V' is the volume element in the transformed space corresponding to the V in the physical space. Re and F are the usual Reynolds number and Froude number respectively. Subscripts of ξ, η, ζ are again representing partial derivatives with respect to ξ, η, ζ accordingly.

Futhermore,

$$J_{12} = x_\xi y_\eta - x_\eta y_\xi$$

$$J = J_{12} / a$$

where a is the ratio of the length of the pipe axis on the transformed plane to that on the physical plane.

It should be noted that in the transformed space, x-momentum depends not only on the pressure gradient in the x-direction, but also on the pressure gradient in the y- and z-directions. This is a unique feature due to the coordinate transformation. Furthermore, in the conventional staggered mesh arrangement for momentum cells, pressures are stored at the grid points and velocities are stored on the grid line between the grid points. This arrangement will require the pressure to be specified on the boundary surface. To avoid this artificial specification, a modified staggered cell arrangement is chosen. In the modified arrangement, velocities are stored at the intersection of grid lines, while pressure, density, and enthalpy are stored at the center of the cells formed by the grid lines. Details of the arrangement can be found in Reference 2.

IV. TEST DESCRIPTION

The experiment was performed at GFK Karlsruhe facility to investigate the fuel assembly behavior after a power outage to the reactor coolant pump coincident with a failure of the reactor to trip. A group of seven heater pins within a hexagonal wrapper was used to represent the fuel pins within a fast reactor fuel subassembly.

Figure 1 shows the axial partitioning and thermocouple locations of the model 7-pin bundle. There is an unheated entrance region 80 mm long. Following that is a heated region of 600 mm. Grids are uniformly spaced along the channel. The sodium coolant enters the assembly with a uniform velocity of 2.15 m/sec and a uniform temperature of 553°C. The rods are uniformly heated by the embedded electric tape. The total heat generated by the rods is 78.6 kW. The inlet velocity drops linearly from 2.15 m/sec to 0.35 m/sec in 6 seconds. Figure 2 shows the flow history. During the transient, part of the heat generated is stored inside the fuel rods. The detailed test arrangements and thermocouple descriptions are given in Reference 3.

V. PHYSICAL MODELS

BODYFIT-1FE code was used for the simulation. It incorporated a one-dimensional fuel pin model to account for the radial heat transfer within the fuel pin. This 1-D fuel pin model is similar to those in Refs. 4 and 5. A constant gap between the fuel and the clad was assumed in the simulation. The gap conductance of 1.30 J/m/sec/°C was used for the simulation. BODYFIT code also includes a grid resistance model to account for the flow redistribution due to the presence of the grids. The pressure drop due to the grid is given by $\Delta P_{grid} = C_v E^2 \frac{1}{2} \rho w^2$ where C_v is the loss coefficient, E is the fraction of the area blocked by the spacer grid, ρ is the density of the fluid, and w is the averaged axial flow velocity. This resistance model is the same as the one used in Reference 6. An empirical correlation for C_v was used i the turbulence flow region.

$$C_v = \frac{27.7}{Re^{0.1233}}$$

Because of the proprietary information on the spacer design, we can only use approximated values for the E's. They are 0.3 for the central subchannel, 0.4 for the wall subchannel and 0.2 for the corner subchannel.

All the heat capacity of the duct wall was included in the simulation. Furthermore, it was found that the temperature distribution was not very sensistive to the variation in values of turbulent viscosity used. Therefore, a simple effective viscosity was used for the simulation instead of more elaborate one-or two-equation turbulence models. As to the conductivity, a simple effective turbulent conductivity was used.

VI. COMPARISON OF RESULTS

The computational meshes before and after the coordinate transformation are given in Figure 3. The dashed line in Figure 3(a) represents the branch cut through which the physical geometry was unwrapped into the transformed geometry 3(b). Figure 4 shows the axial velocity distributions along two vertical cross sections AA and BB of Figure 3(a). Figure 5 gives the comparison between the code prediction and the experiment values for the steady state temperature distribution. The agreements are, in general, very good. Figure 6 shows the radial temperature distribution along sections AA and BB of Figure 3. It also shows the fuel pin structure and their dimensions. Figures 7 through 20 give the measured and the calculated thermocouple readings for various levels and locations. The slope of the calculated temperature is slightly larger than the measured temperature during the transient. This slope is depending on the heat transfer coefficient at the clad surface, the gap conductance between the fuel and the clad, the averaged heat conductivity for the fuel region, etc. The agreements could be improved through more accurate modeling of these data.

VII. CONCLUSION

BODYFIT-1FE was used to simulate the 7-pin flow rundown experiment. The results of the comparison between the code prediction and the measured value are very encouraging. The agreement can be improved by refining the heat transfer coefficients and physical models. Most importantly it demonstrates the capability of the BODYFIT code in providing detailed velocity and temperature distributions in a reactor rod bundle. This information is essential for ascertaining empirical coefficients used in subchannel codes. The same experiment was also simulated by COMMIX-1A.[7] The predictions between BODYFIT and COMMIX are fairly close. However, because of the porous medium formulation used in COMMIX code, it requires empirical coefficients such as the distributed resistance be specified as inputs to the code. The BODYFIT-1FE code is a bench mark code since it does not invoke any assumptions and empirical coefficients for the laminar flow case. All the conservation equations are rigorously treated except for the case of turbulent flow where a turbulent flow model is needed for the closure of the differential equations. Furthermore, due to the fine computational grids used in BODYFIT, it is possible to make direct one-to one-comparison between the BODYFIT predictions and the experimental data, whereas COMMIX requires great care in interpolating and averaging of the calculated values. These averaged values could be sensitive to the weighting factors used. The capability to analyze two-phase flow is to be added into BODYFIT, which will further increase the applicability of the code for various thermal hydraulic analysis.

ACKNOWLEDGEMENTS

The authors want to thank Miss B. D. Wright for typing the manuscript, Drs. R. T. Curtis, C. N. Kelber and P. M. Wood of the United States Nuclear Regulatory Commission for their support and encouragement and Drs. W. Peppler, and A. Kaiser (KFK, Germany) for their help in providing the detailed experimental data used in this report.

References

1. W. T. Sha and J. F. Thompson, "Rod Bundle Thermal-Hydraulic Analysis Using Boundary Fitted Coordinate System," NUREG/CR-0001, ANL-78-1 (Jan 1979).

2. B. C-J. Chen, W. T. Sha, M. L. Doria, R. C. Schmitt, and J. F. Thompson "BODYFIT-1FE, A Computer Code for Three Dimensional Steady-State/Transient Single Phase Rod Bundle Thermal-Hydraulic Analysis," to be published as an ANL report.

3. I. Aberle, A. J. Brooke, W. Peppler, H. Rohrbacher, K. Schleisiek, "Sodium Boiling Experiments in a 7-Pin Bundle under Flow Rundown Conditions," KFK-2378, Institut fur Reaktorentwicklung Karlsruhe, Germany (Nov 1976).

4. F. E. Dunn, G. J. Fischer, T. J. Heames, P. A. Pizzica, N. A. NcNeal, W. R. Bohl, and S. M. Prastein, "The SAS2A LMFBR Accident-Analysis Computer Code," ANL-8138 (Oct 1974).

5. W. T. Sha, H. M. Domanus, R. C. Schmitt, J. J. Oras, and E. I. H. Lin, "COMMIX-1: A Three-Dimensional Transient Single-Phase Component Computer Program for Thermal-Hydraulic Analysis," NUREG/CR-0415, ANL-77-96 (Sept 1978)

6. Klaus Rehme, "Pressure Drop Correlations for Fuel Element Spacers," Nuclear Technology, Vol. 17 (Jan 1973).

7. H. M. Domanus, M. J. Chen, W. T. Sha, "Computational Results for a 7-Pin Hexagonal Fuel Assembly during a Flow Rundown Transient Using the COMMIX 1A Computer Code," NUREG/CR-1285, ANL-CT-80-10 (Jan 1980).

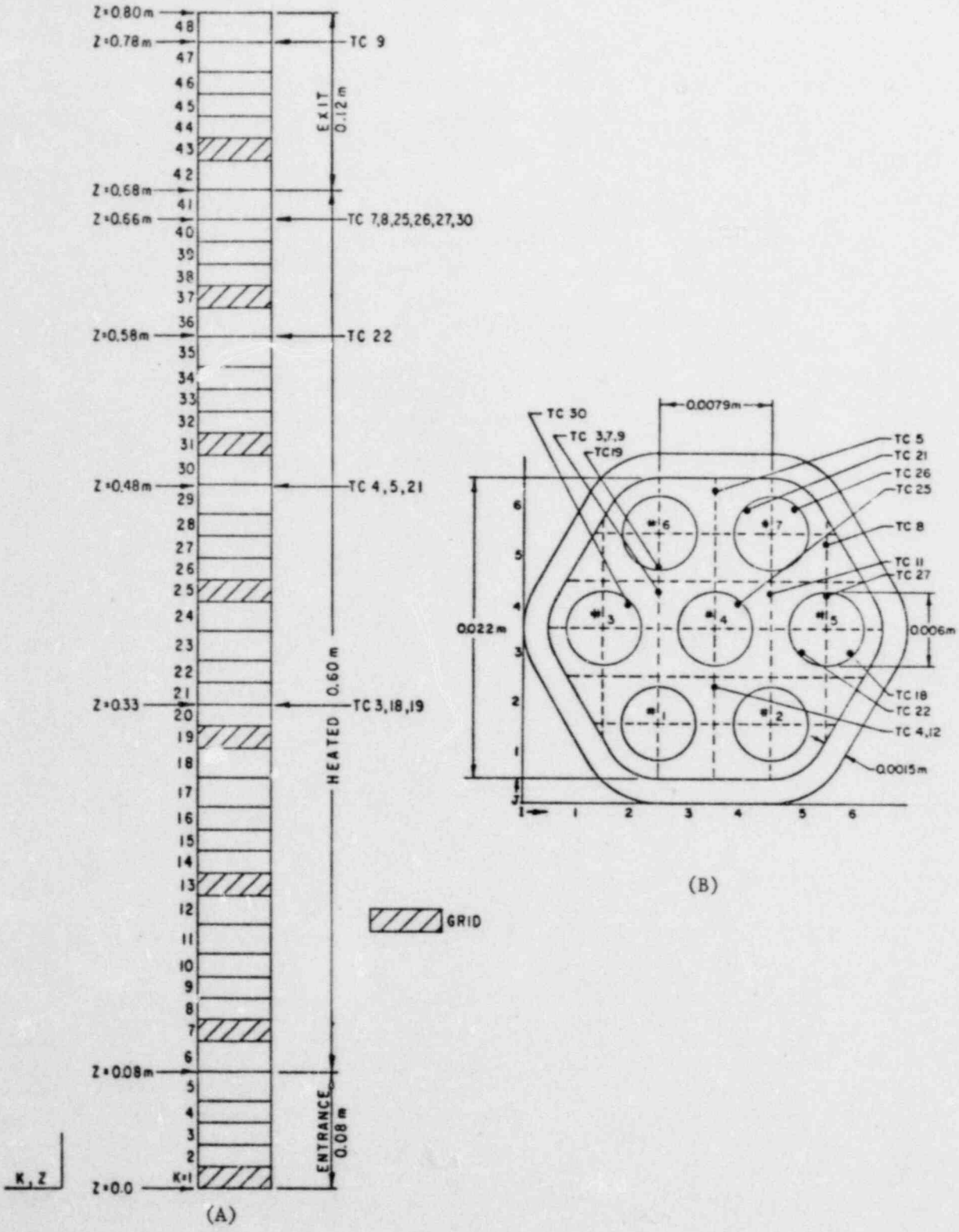

Fig. 1. (A) Axial Partitioning and (B) Thermocouple Locations of Model 7-Pin Bundle ANL Neg. No. 116-80-139

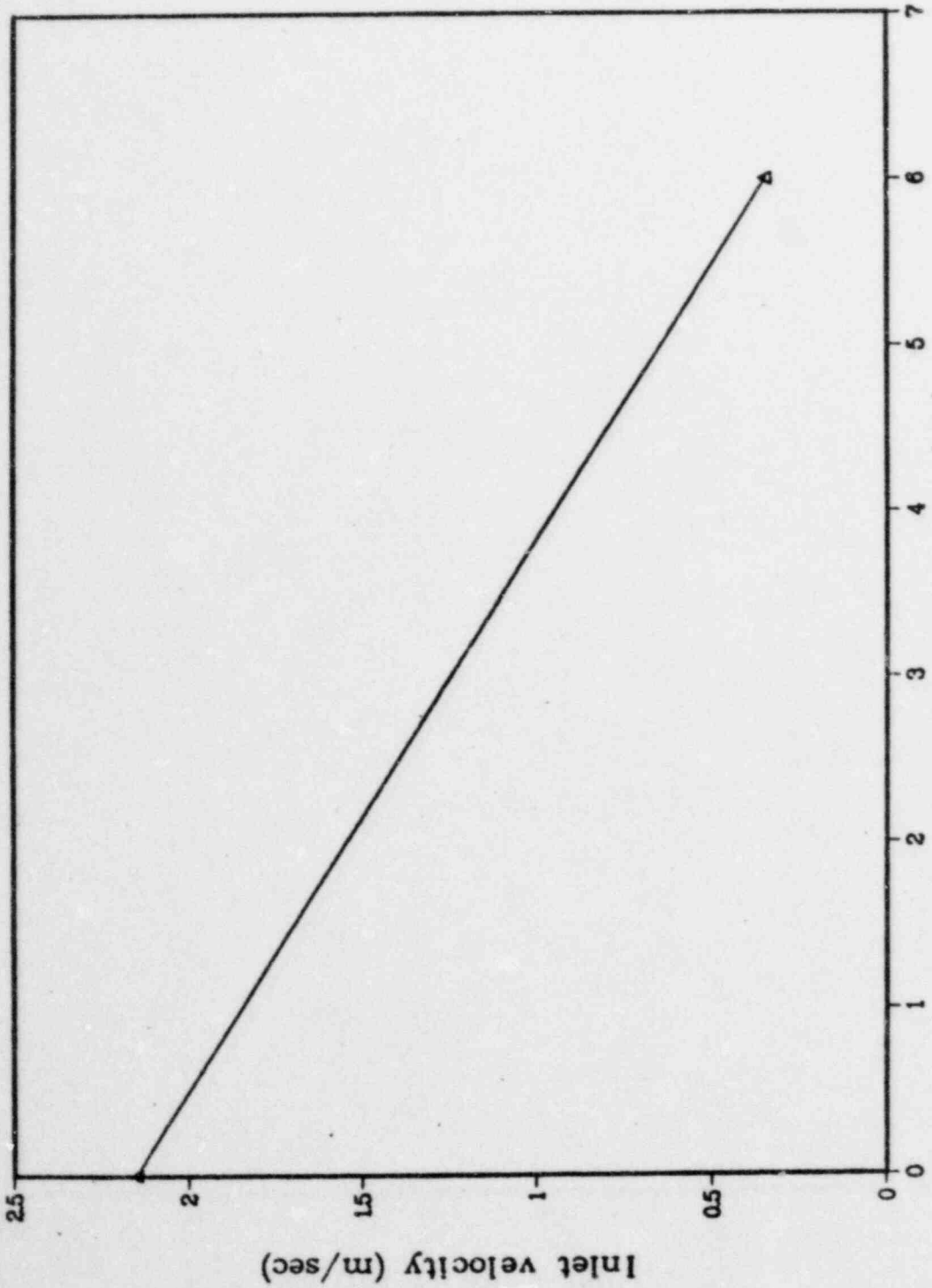

Fig. 2. Flow History during the Transient

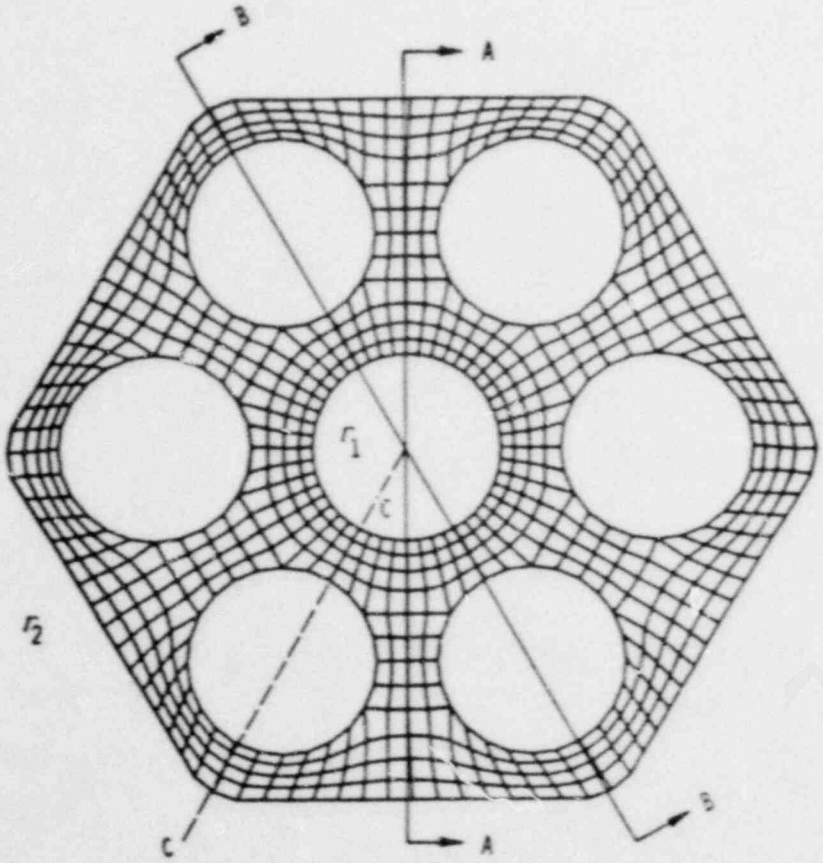

RADIUS = 3.0 mm
GAP BETWEEN PINS = 1.9 mm
FLAT TO FLAT = 22 mm
V_m = 2.15 m/s
Re = 3.373×10^4
HEAT FLUX = $.993 \times 10^6$ WATTS/m^2

(a)

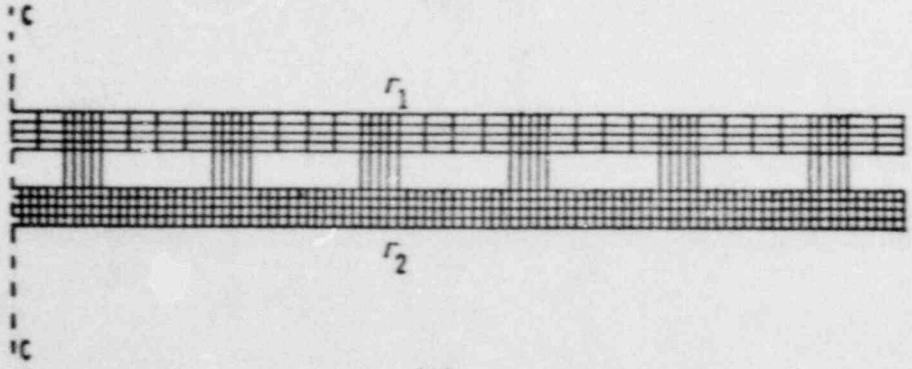

(b)

Fig. 3. (a) Physical Plane and Dimensions, (b) Transformed Plane. ANL Neg. No. 116-79-192R1.

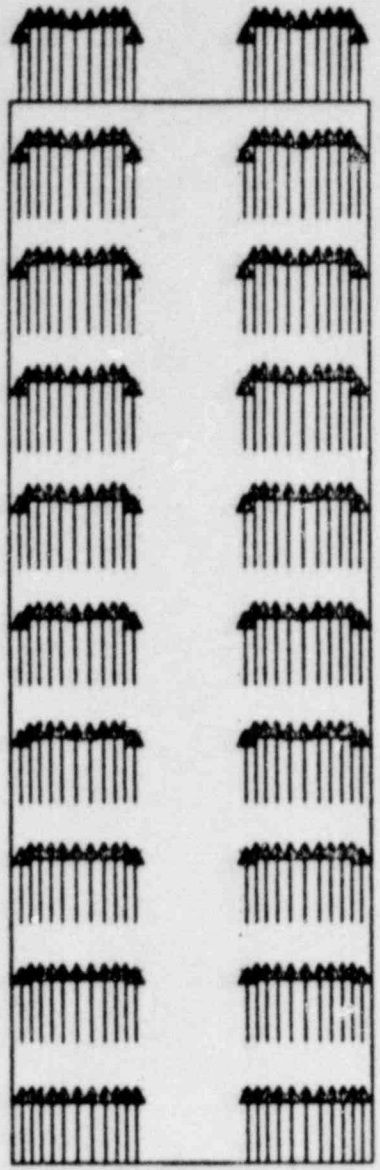

Fig. 4(a). Axial Velocity along Section AA

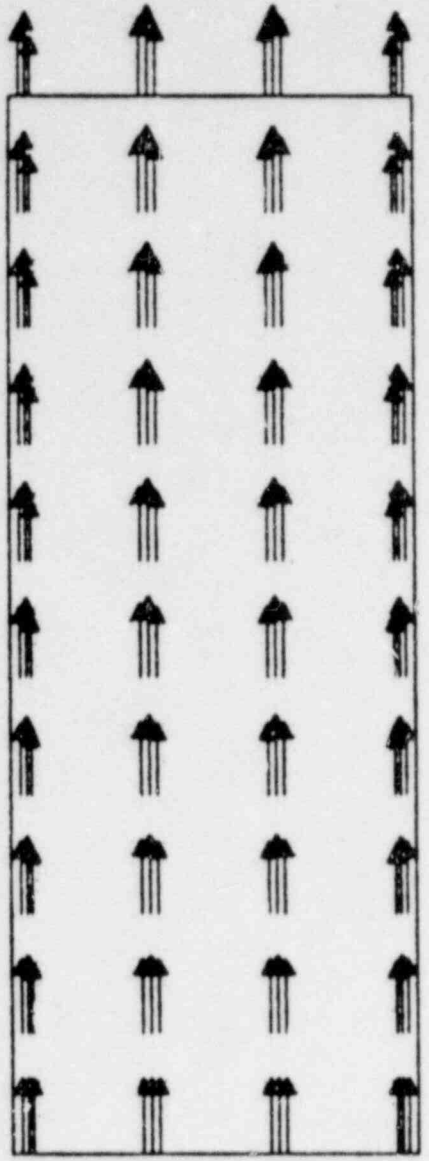

Fig. 4(b). Axial Velocity along Section 3B

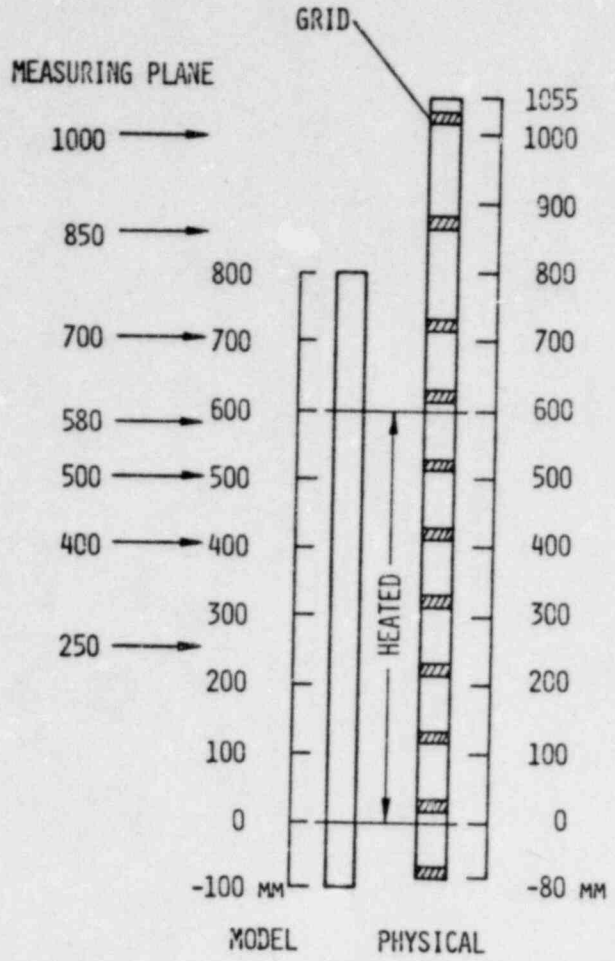

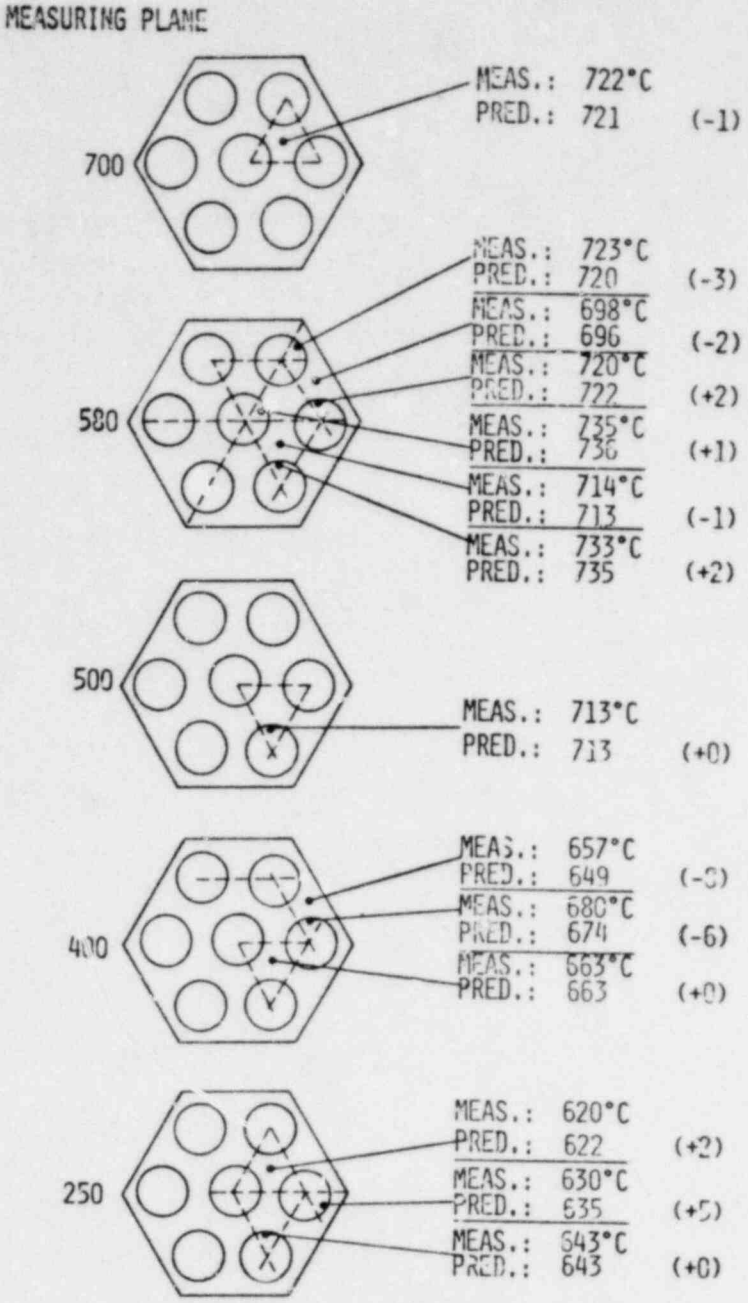

Fig. 5. Comparison of Steady State Temperature Distributions

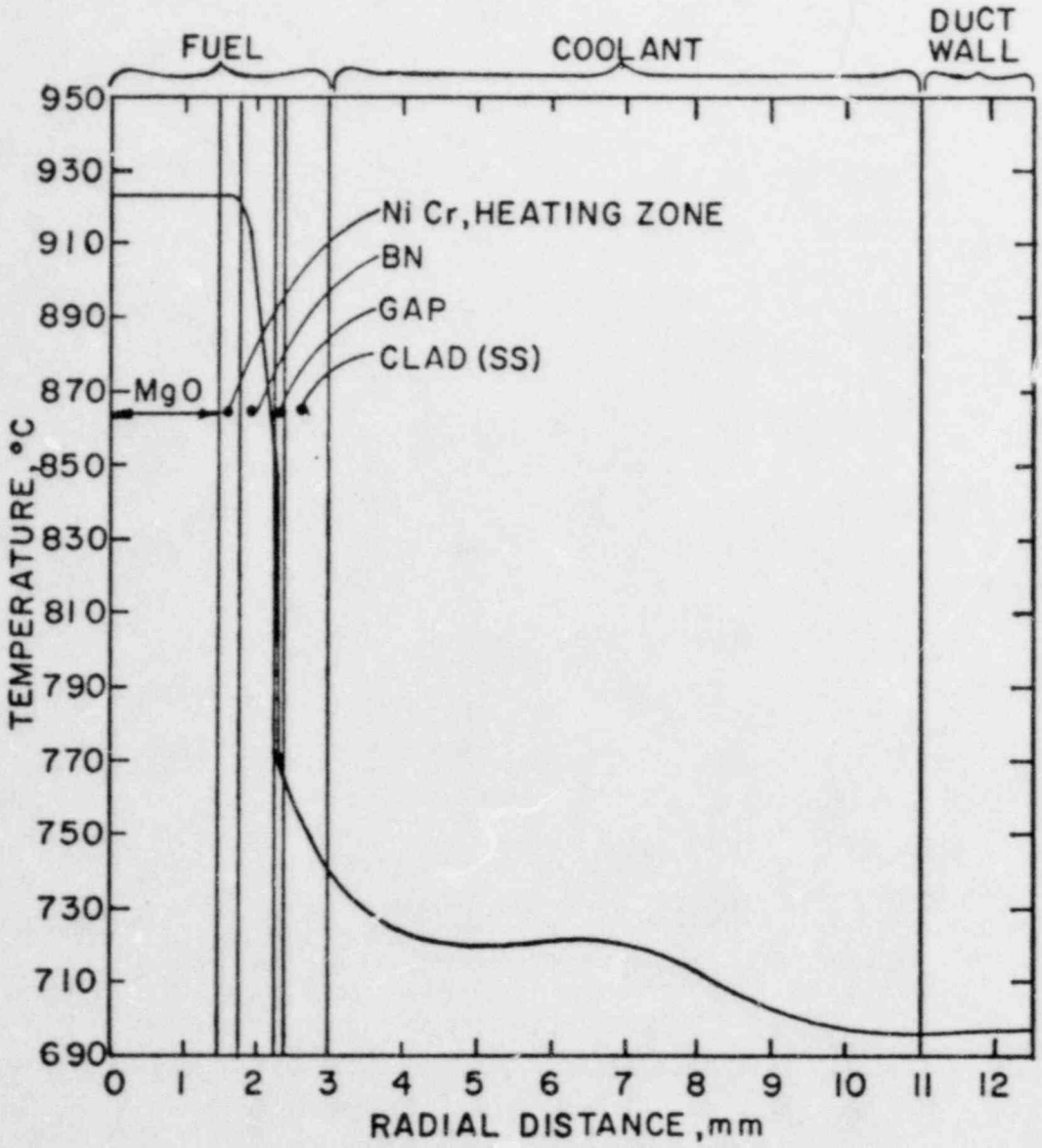

Fig. 6(a). Radial Temperature Distribution along Section AA of Fig. 3

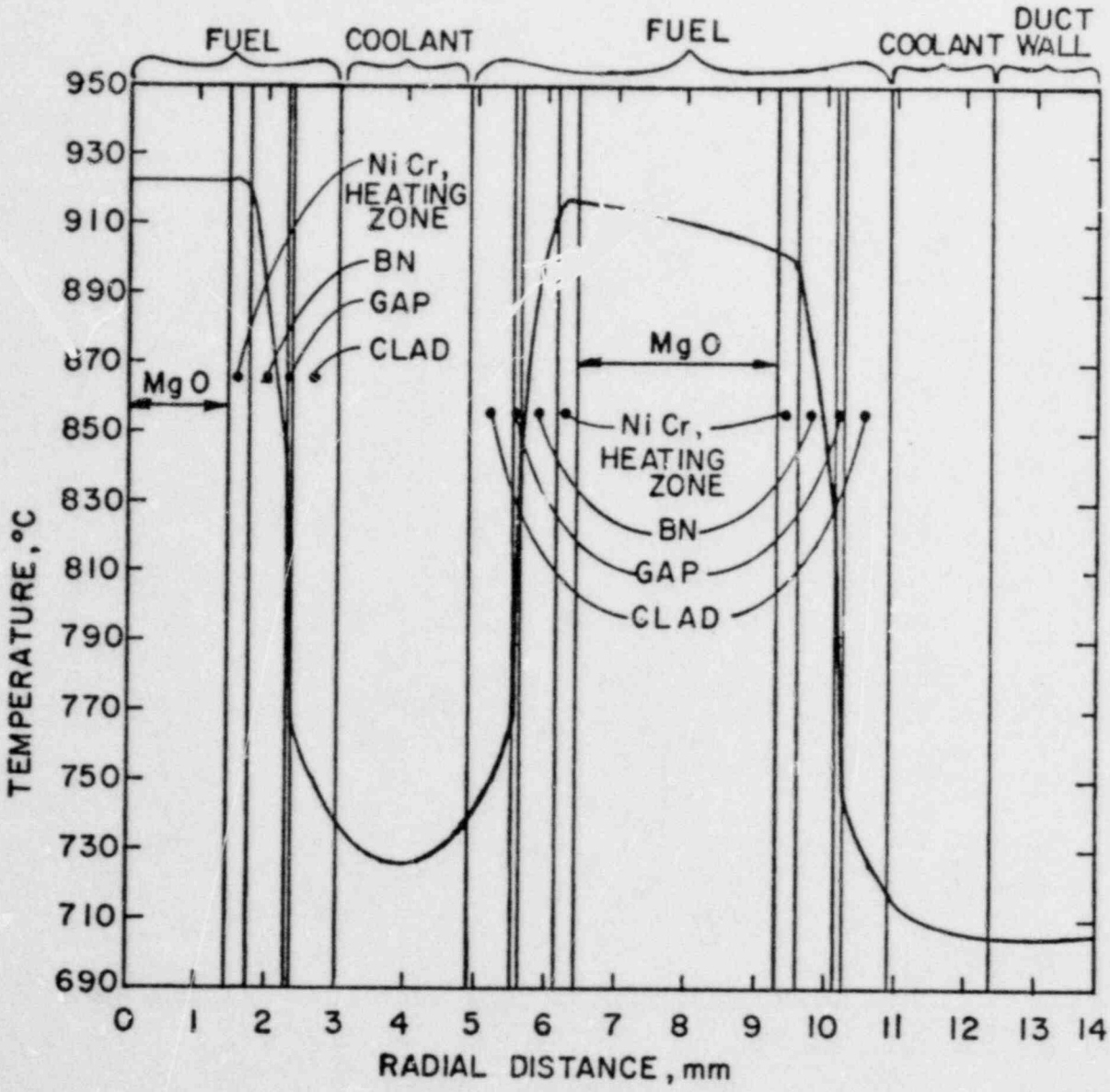

Fig. 6(b). Radial Temperature Distribution along Section BB of Fig. 3.

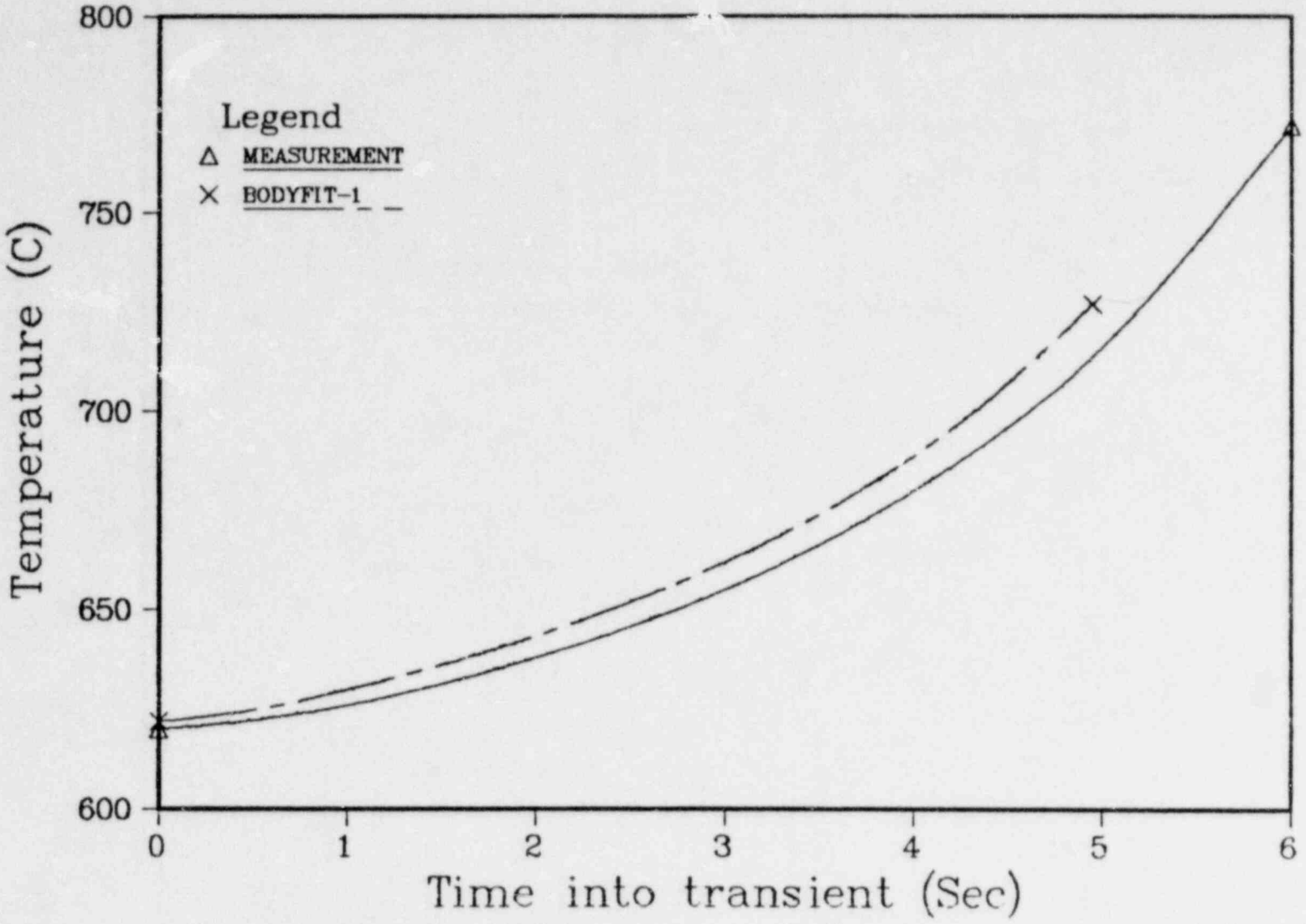

Fig. 7. Comparison of Temperature during Transient for Thermocouple TC 3

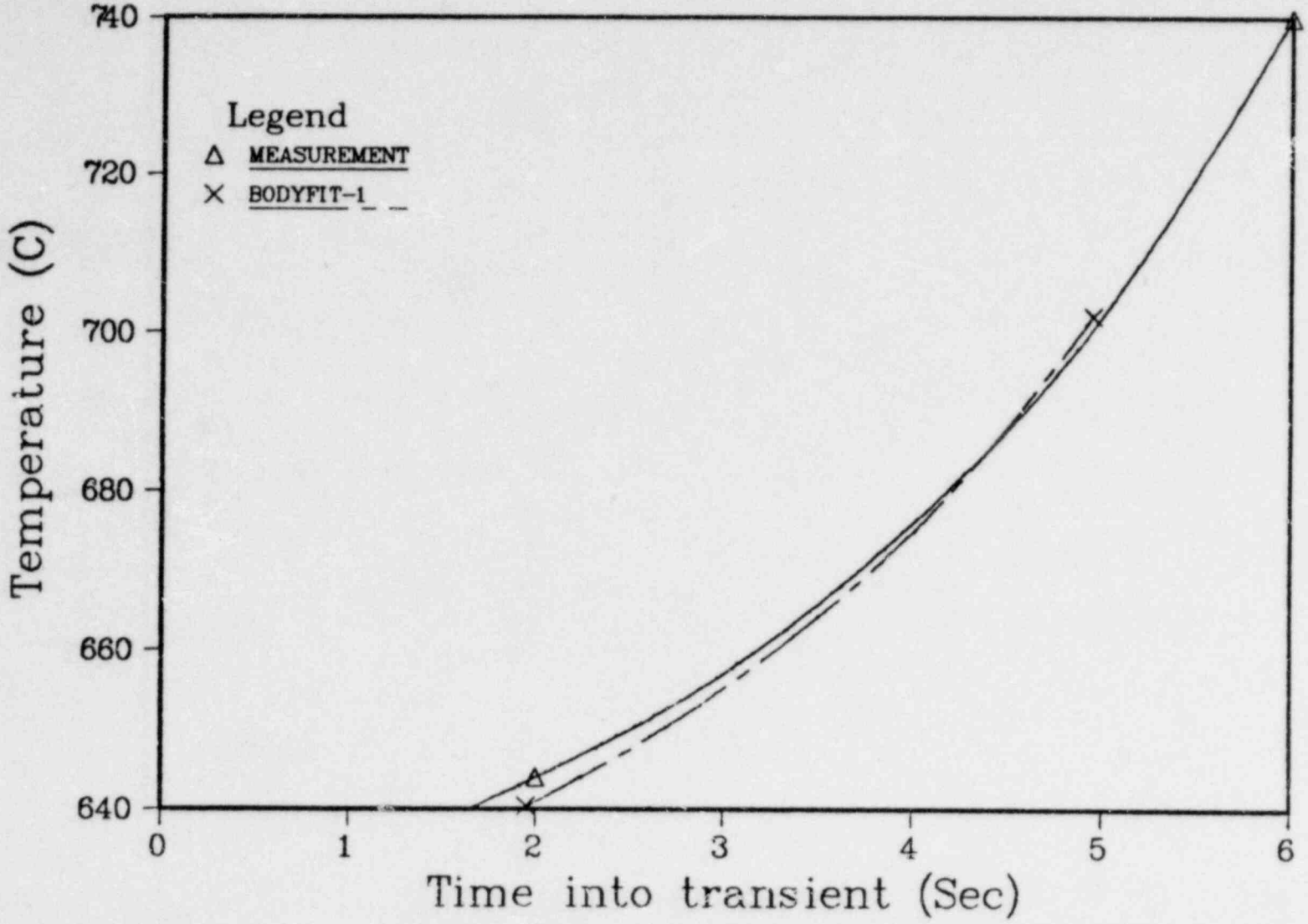

Fig. 8. Comparison of Temperature during Transient for Thermocouple TC 18

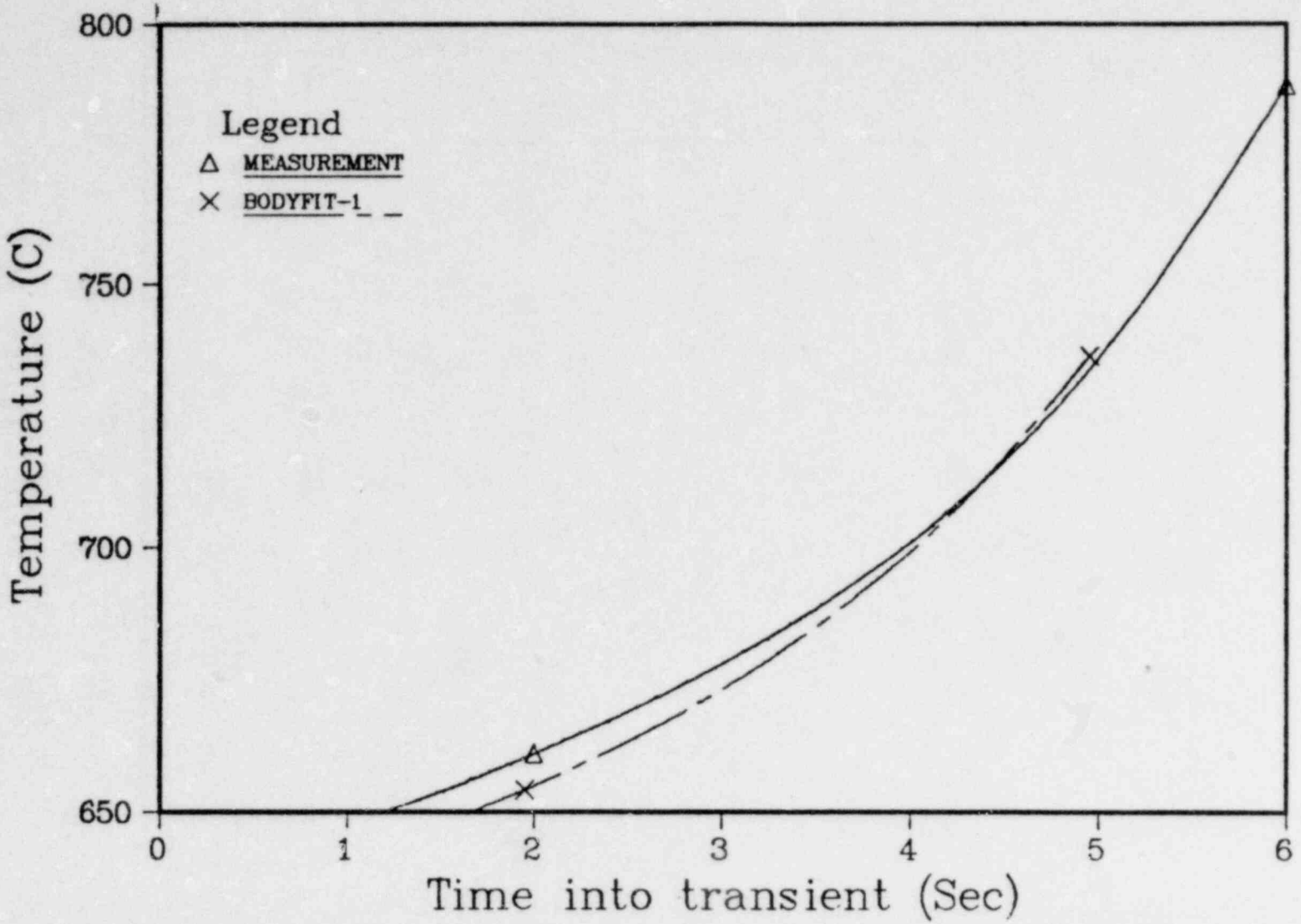

Fig. 9. Comparison of Temperature during Transient for Thermocouple TC 19

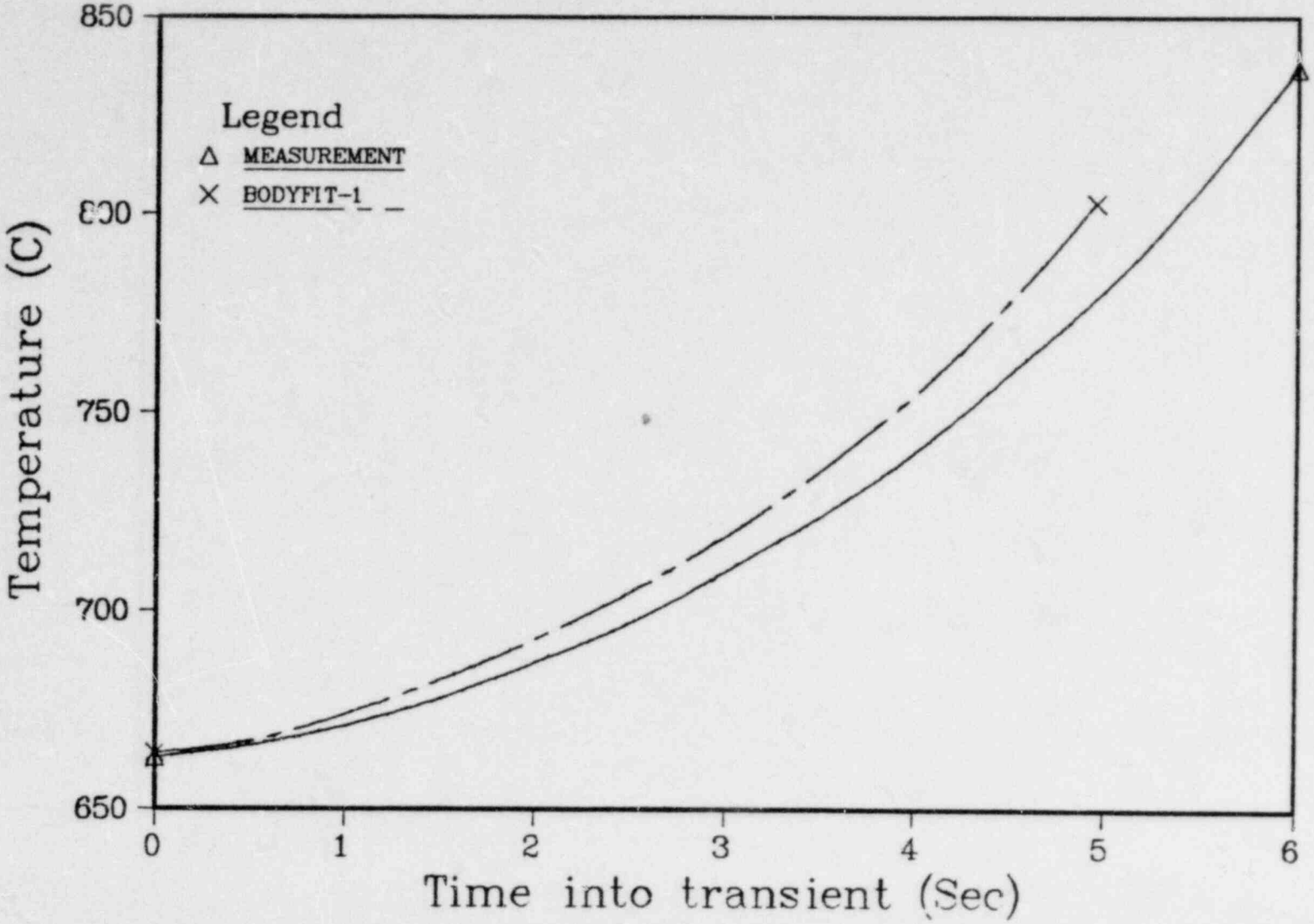

Fig. 10. Comparison of Temperature during Transient for Thermocouple TC 4

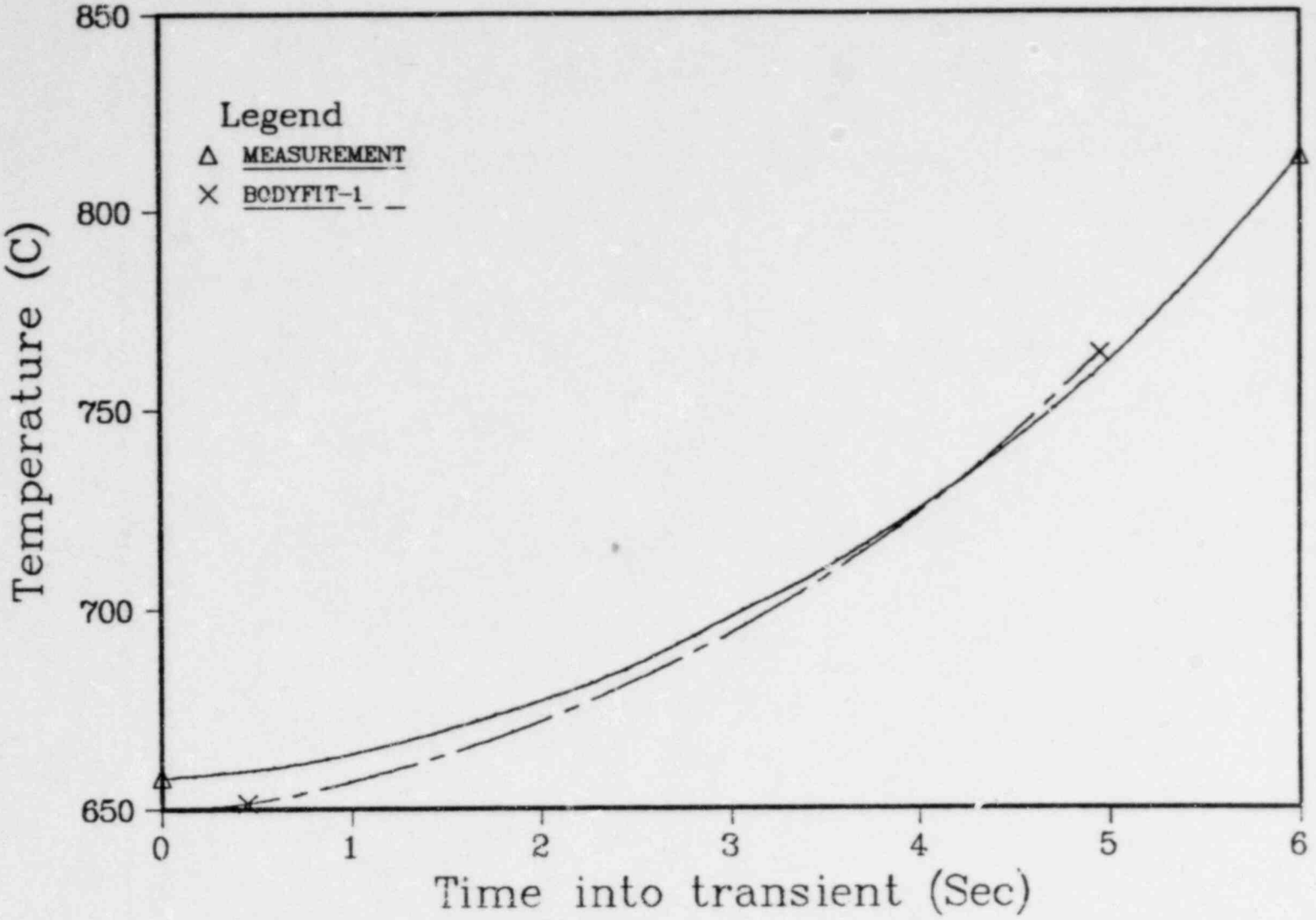

Fig. 11. Comparison of Temperature during Transient for Thermocouple TC 5

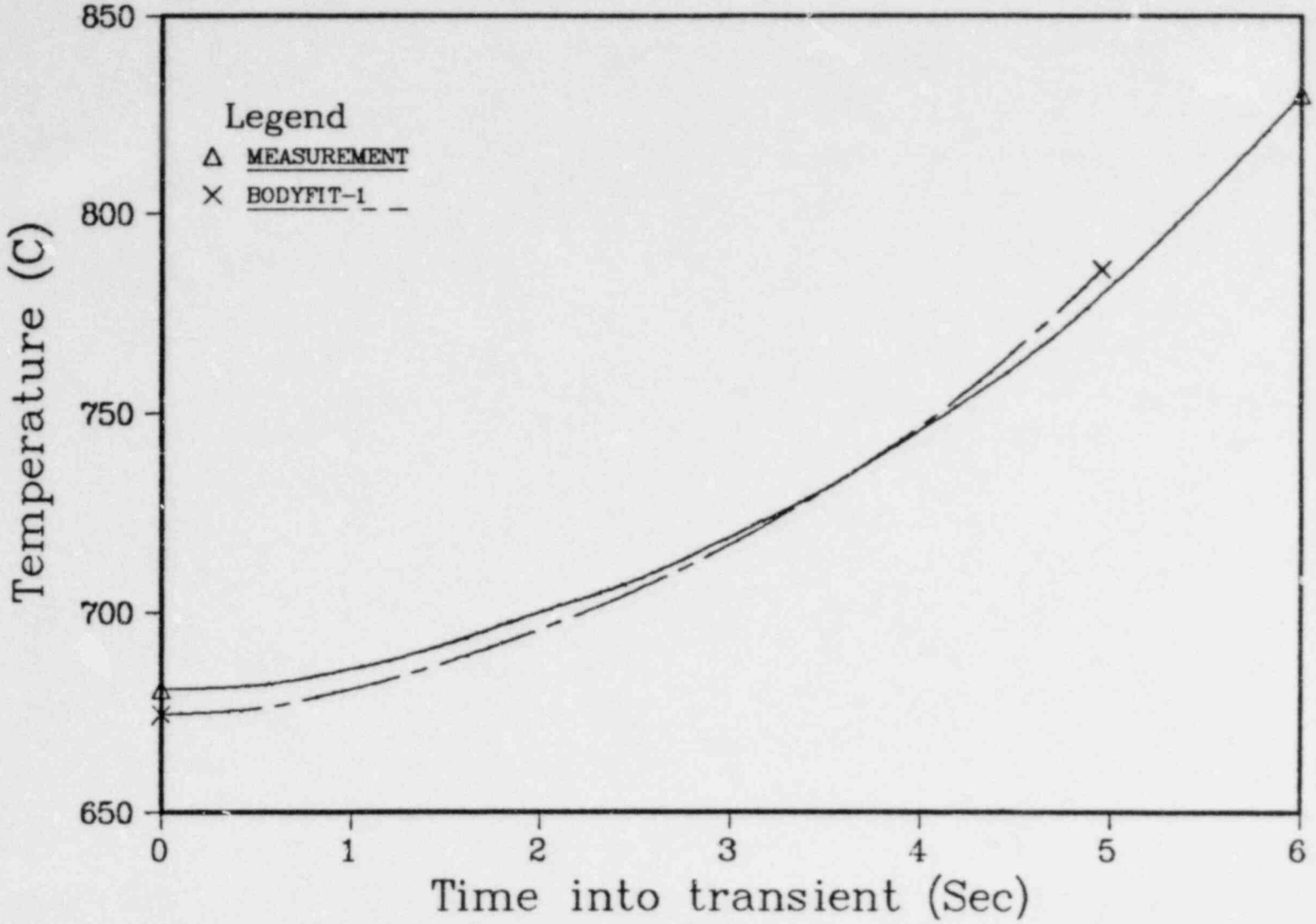

Fig. 12. Comparison of Temperature during Transient for Thermocouple TC 21

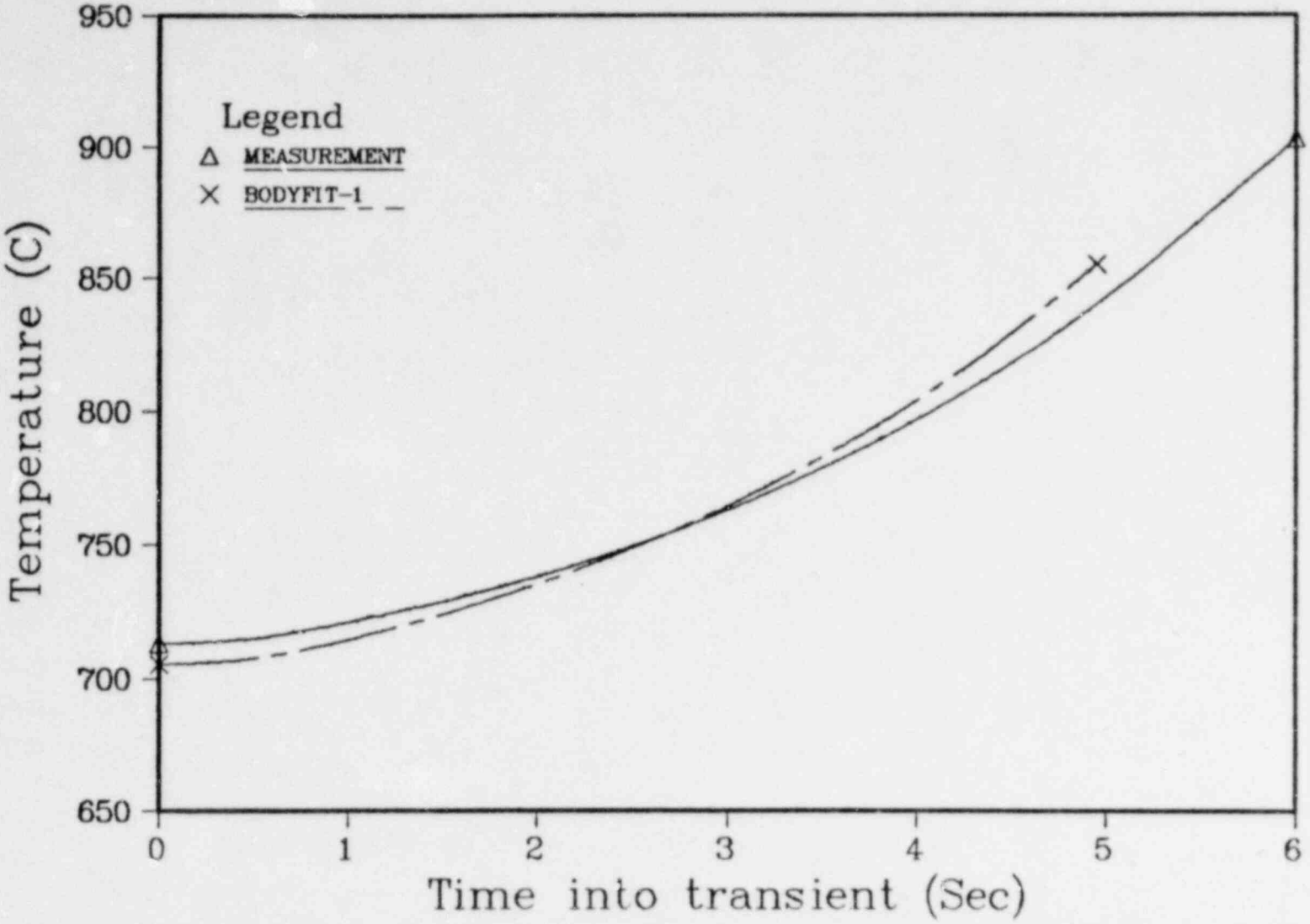

Fig. 13. Comparison of Temperature during Transient for Thermocouple TC 22

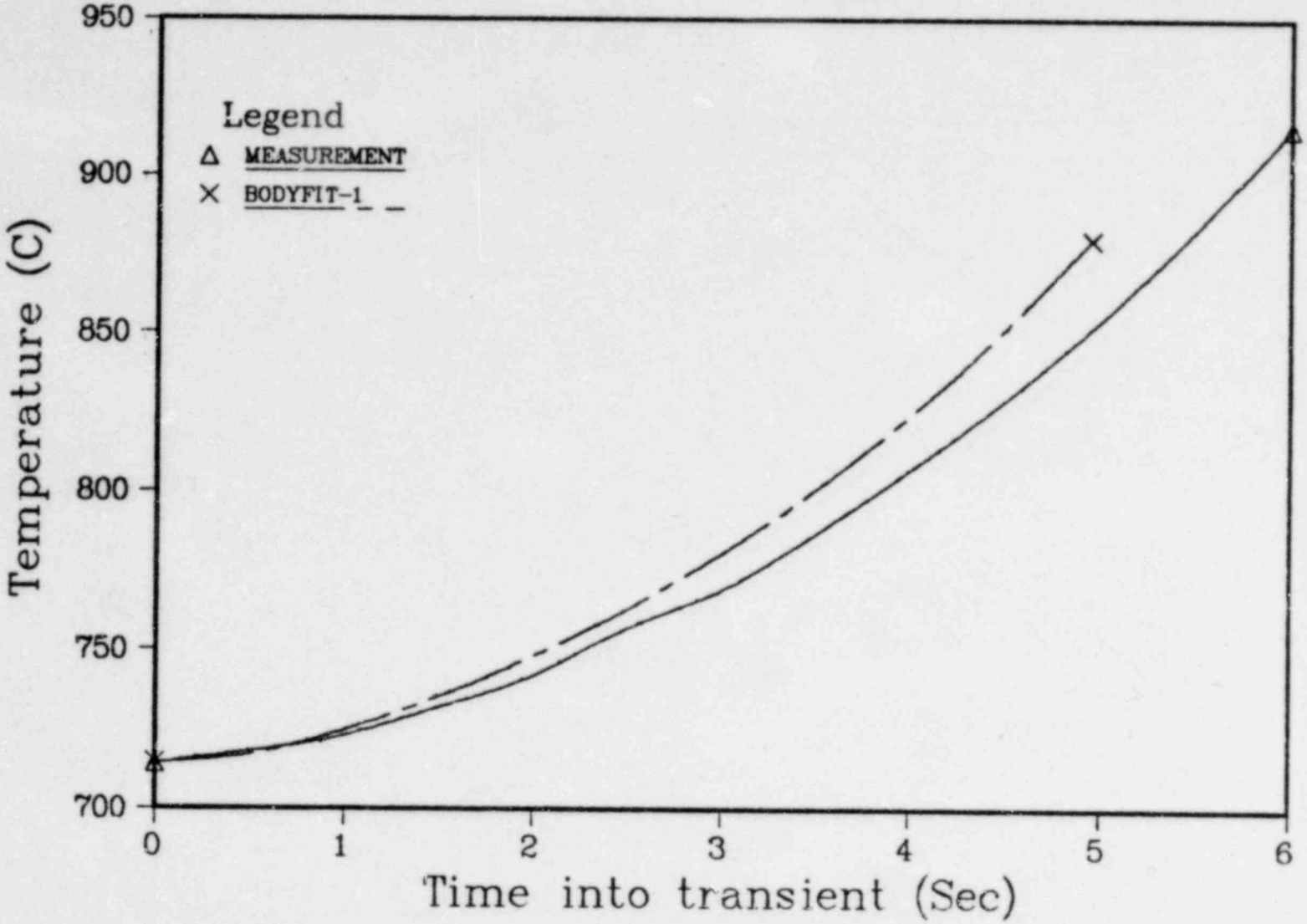

Fig. 14. Comparison of .emperature during Transient for Thermocouple TC 7

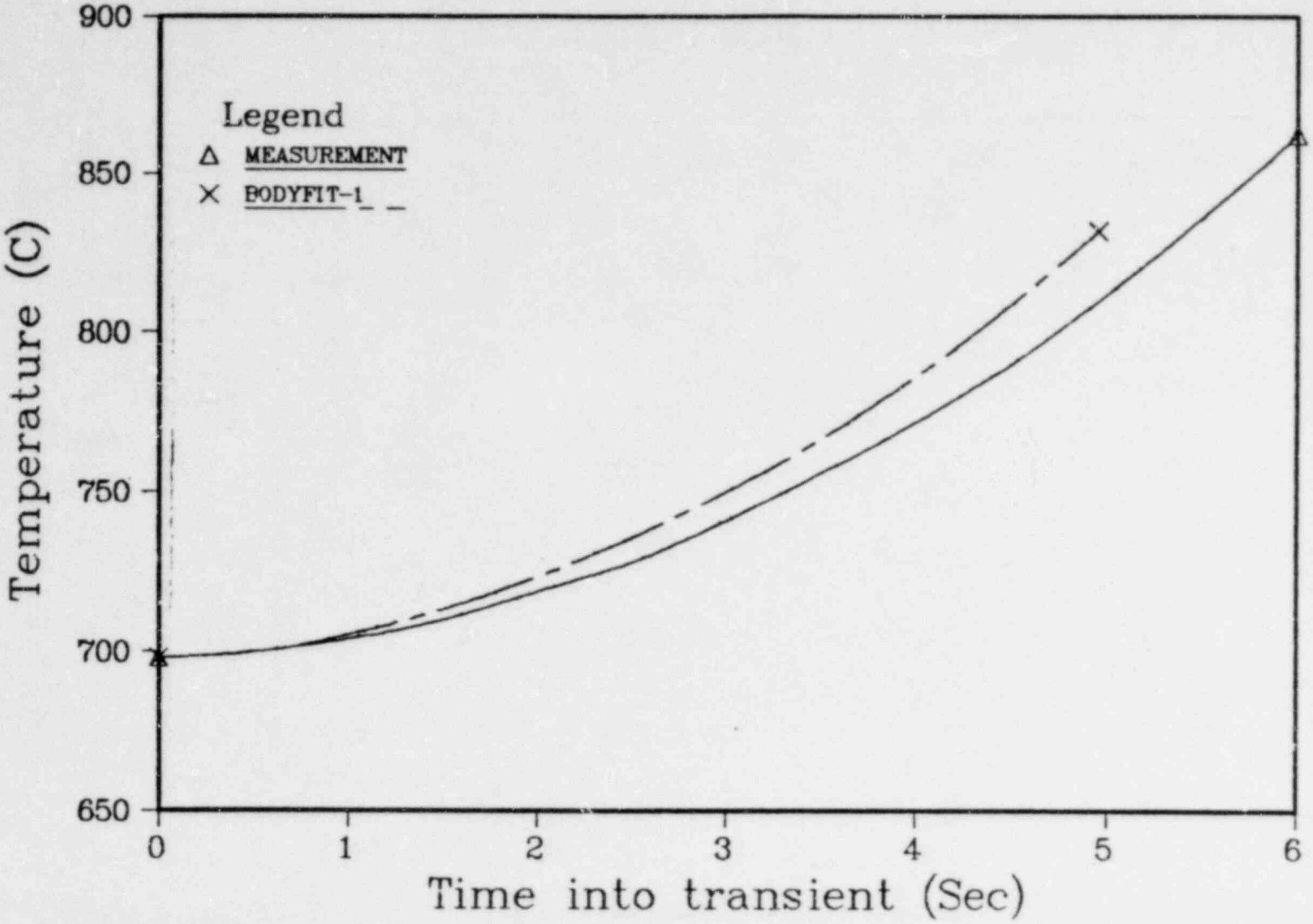

Fig. 15. Comparison of Temperature during Transient for Thermocouple TC 8

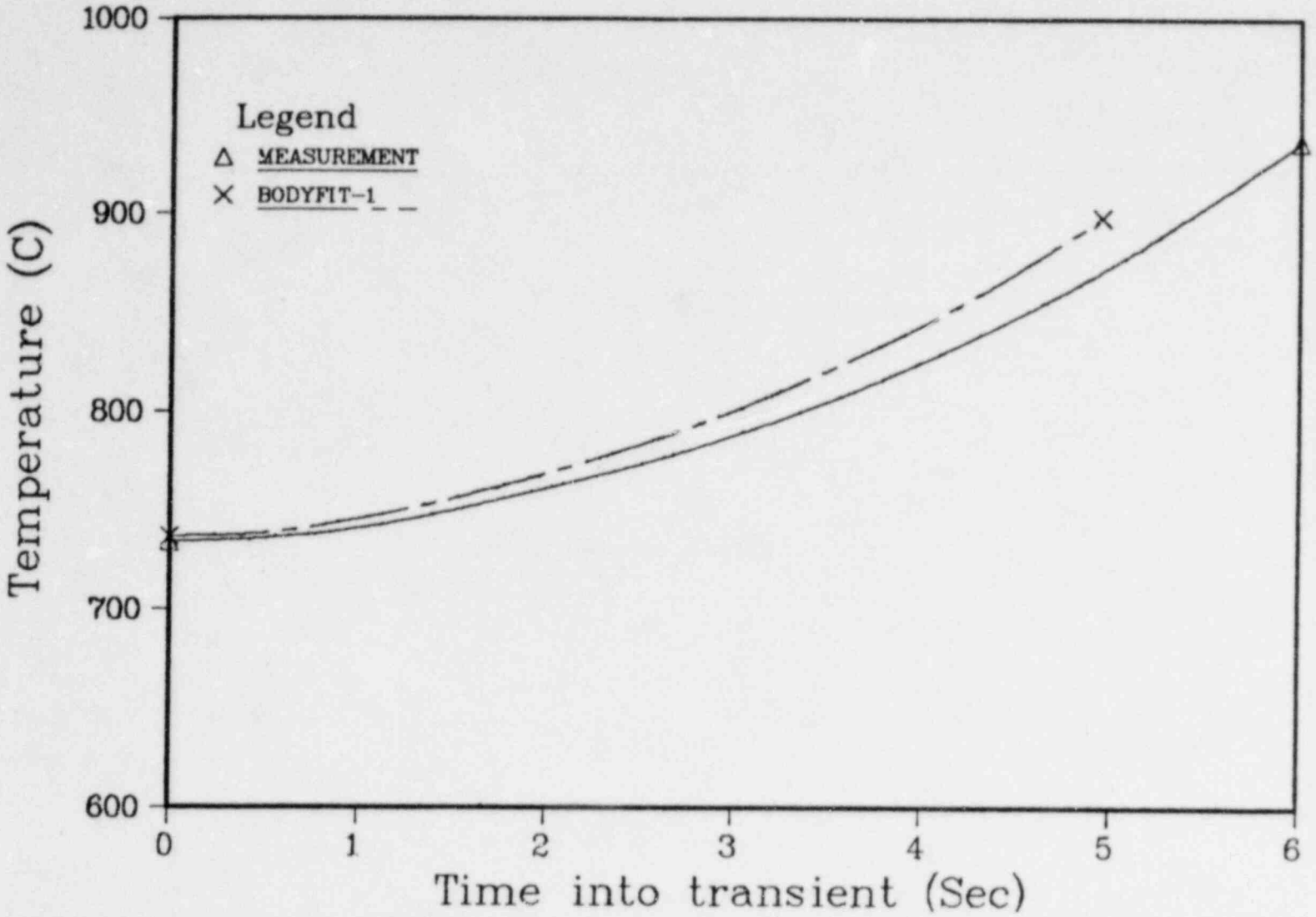

Fig. 16. Comparison of Temperature during Transient for Thermocouple TC 25

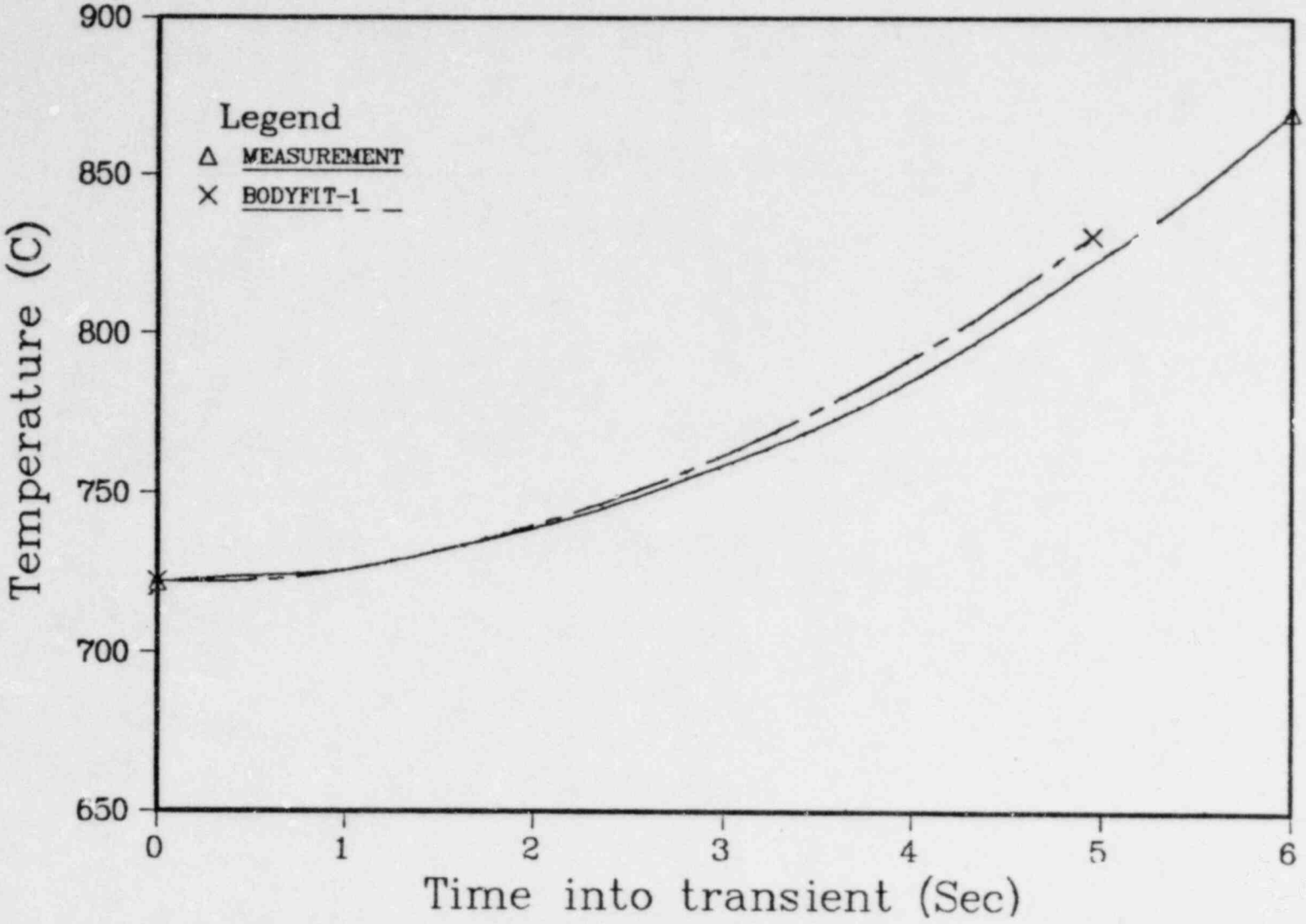

Fig. 17. Comparison of Temperature during Transient for Thermocouple TC 26

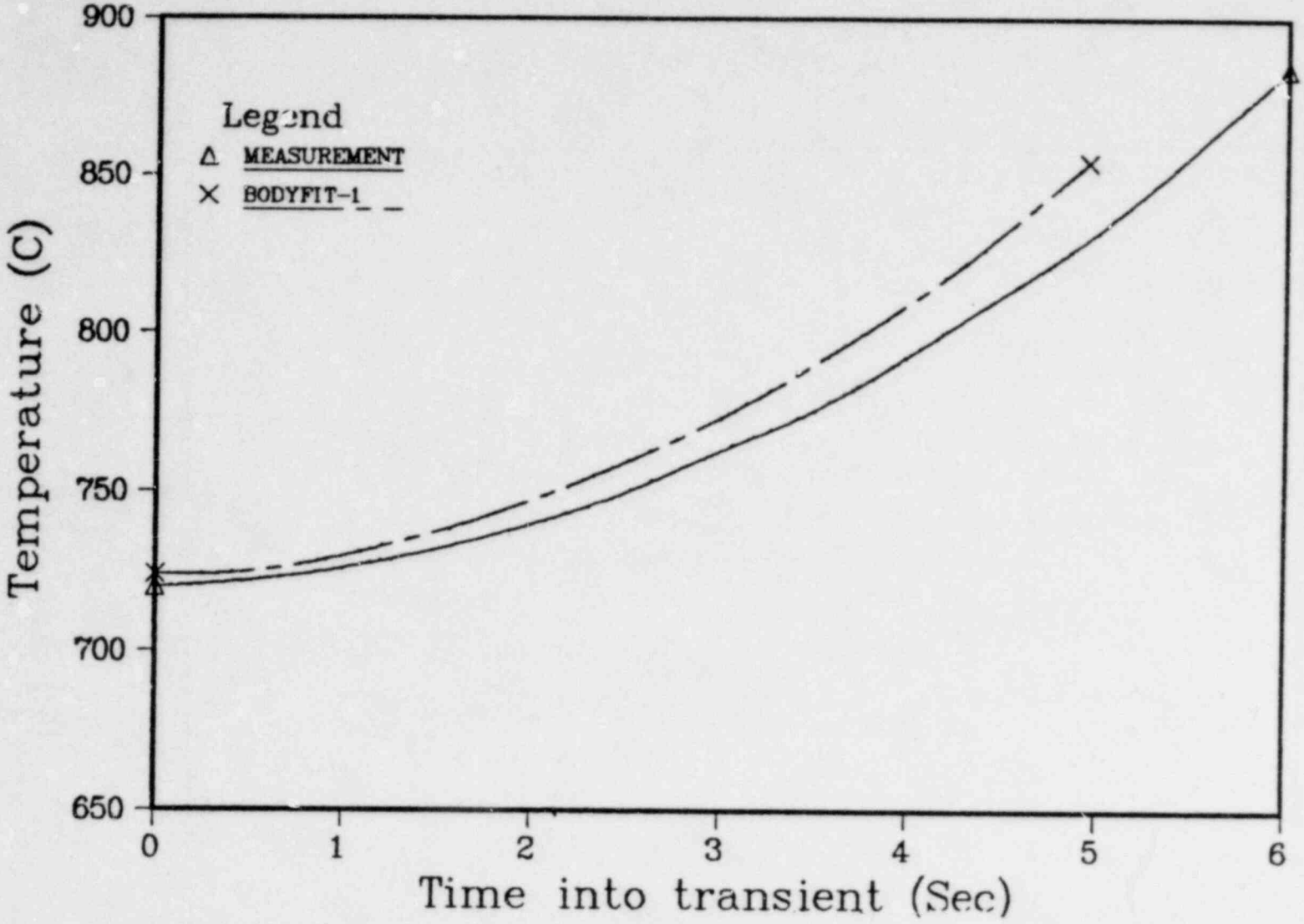

Fig. 18. Comparison of Temperature during Transient for Thermocouple TC 27

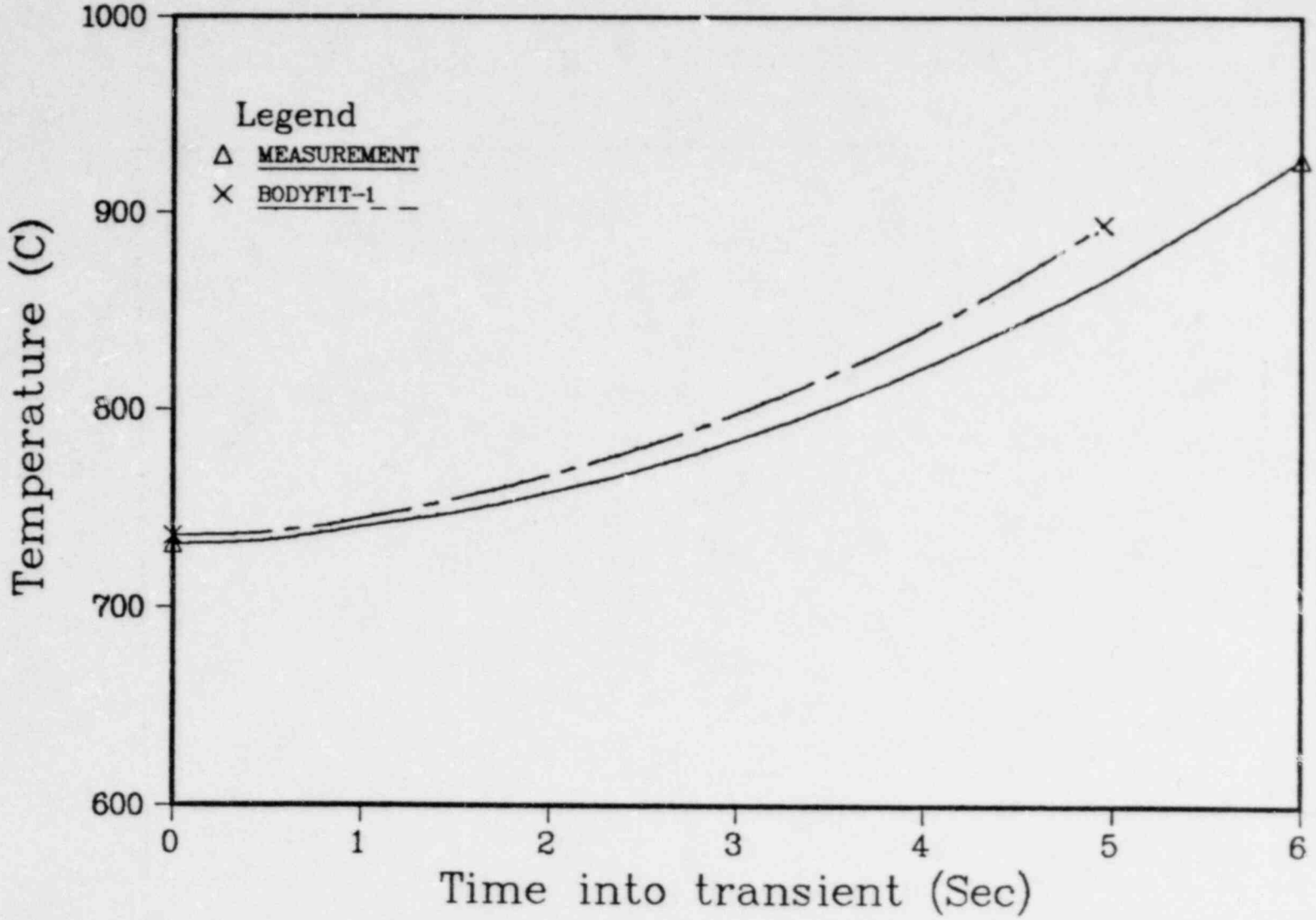

Fig. 19. Comparison of Temperature during Transient for Thermocouple TC 30

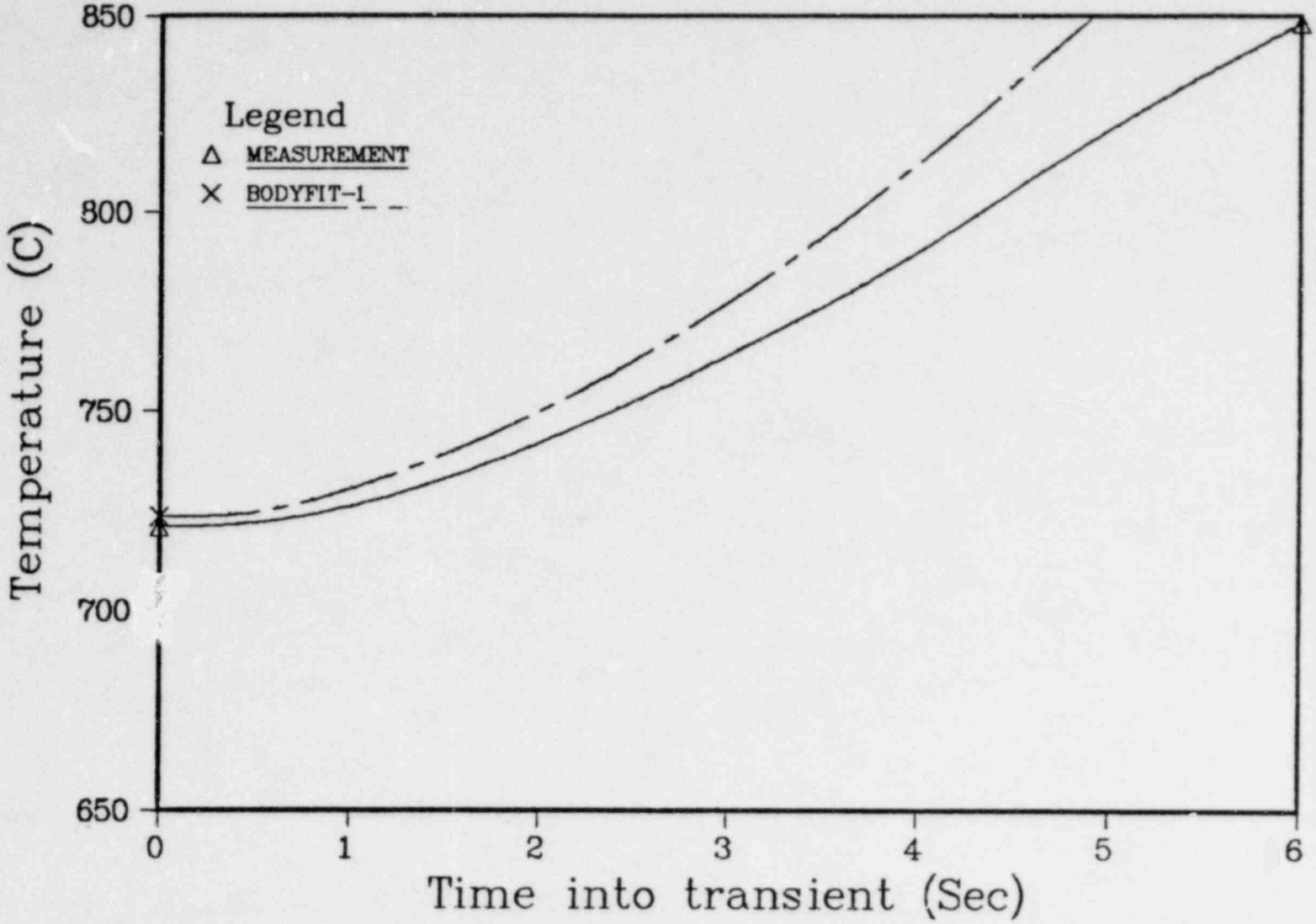

Fig. 20. Comparison of Temperature during Transient for Thermocouple TC 9

Distribution for NUREG/CR-1814 (ANL-CT-81-9)

Internal:

E. S. Beckjord
C. E. Till
R. S. Zeno
P. R. Huebotter
G. S. Rosenberg
Y. S. Cha
B. C-J. Chen (10)
T. H. Chien
H. M. Domanus
J. R. Hull
C. C. Miao
R. C. Schmitt
W. T. Sha (10)
V. L. Shah
Y. W. Shin
M. Weber
C. I. Yang
M. Ishii
D. R. Ferguson
R. M. Singer
G. K. Leaf
P. L. Garner
D. P. Weber
P. B. Abramson
H. H. Hummel
J. Sanecki
ANL Contract File
ANL Libraries (2)
TIS Files (3)

External:

NRC, for distribution per R7 (380)
DOE-TIC (2)
Manager, Chicago Operations and Regional Office, DOE
Chief, Office of Patent Counsel, DOE-CORO
President, Argonne Universities Association:
Components Technology Division Review Committee:
F. W. Buckman, Consumers Power Co., Jackson, Mich. 49201
P. F. Cunniff, U. Maryland, College Park, Md. 20742
R. A. Greenkorn, Purdue U., West Lafayette, Ind. 47907
W. M. Jacobi, Westinghouse Electric Corp., Pittsburgh, Pa. 15230
M. A. Schultz, North Palm Beach, Fla. 33408
A. Sesonske, Purdue U., West Lafayette, Ind. 47907
J. Weisman, U. Cincinnati, Cincinnati, O. 45221